JOC The Journal of Organic Chemistry

Article

pubs.acs.org/joc

Nonplanar Organic Sensitizers Featuring a Tetraphenylethene Structure and Double Electron-Withdrawing Anchoring Groups

Fangshuai Zhang,[†,‡] Jie Fan,[†] Huijuan Yu,[†] Zhuofeng Ke,[†] Changming Nie,[‡] Daibin Kuang,*[,†] Guang Shao,*[,†] and Chengyong Su[†]

[†]School of Chemistry and Chemical Engineering, Sun Yat-sen University, Guangzhou, 510275, PR China

[‡]School of Chemistry and Chemical Engineering, University of South China, Hengyang, 421001, PR China

Supporting Information

ABSTRACT: Two metal-free organic sensitizers containing two *N*,*N*-diethylaniline (DEA) moieties and a twisted 1,1,2,2-tetraphenylethene (TPE) structure, dye **SD** with one anchoring group and dye **DD** with two anchoring groups, were synthesized and applied in dye-sensitized solar cells (DSSCs). The introduction of a nonplanar TPE structure was used to form a series of propeller-like structures and reduce the tendency of dyes to randomly aggregate on TiO_2 surface, but without importing an aggregation-induced emission (AIE) property. The thermal stabilities, UV−vis absorption spectra, electrochemical properties, and photovoltaic parameters of DSSCs with these two dyes were systematically studied and compared with each other. The overall conversion efficiencies (η) of 4.56% for dye **SD** and 6.08% for dye **DD** were obtained under AM 1.5 G irradiation.

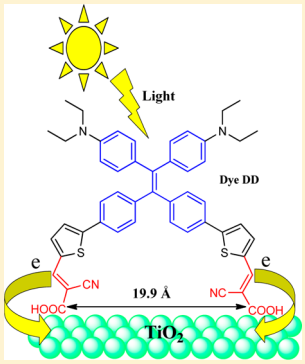

INTRODUCTION

Since the seminal paper reported by O'Regan and Grätzel in 1991,[1] dye-sensitized solar cells (DSSCs) have evolved to be a potential candidate for the next-generation photovoltaic devices. As a critical component in DSSCs, the sensitizer provides electron injection into the conduction band of an oxide semiconductor (e.g., TiO_2) after light excitation and plays a crucial role in increasing the light-harvesting efficiency.[2,3] Although the validated conversion efficiencies of up to 13.0% and 11.1% were achieved by employing Zn- and Ru-based complexes,[4,5] respectively, they have encountered bottleneck problems such as limited resources, environmental pollution, and difficult purification.[6] Recently, many efforts have been made to develop the metal-free organic dye sensitizers due to their high molar absorption coefficients, low costs, and enormous versatility.[7−9] Over the past two decades, tremendous research has been focused on the search for such kind of sensitizers with desired physical properties, such as broad and intense absorption, well-aligned energy levels, and suppressed amorphous aggregation tendency.[10−12] In the design of metal-free organic dye sensitizers, the dipolar donor-(π-conjugated spacer)-acceptor (D−π−A) system is the most widely adopted molecular architecture. The spectral features of D−π−A systems are associated with the intramolecular charge-transfer (ICT) excitation from the donor to the acceptor moiety and are, thus, beneficial for improving their light-harvesting abilities.[13−17]

Unfavorable dye aggregation on the semiconductor surface should be avoided by optimizing the molecular structure of the dye or addition of coadsorbers.[10−12] Ideally, the dye should form a closely packed monolayer, blocking contact between the redox mediator and the semiconductor surface.[2] However, aggregation is an intrinsic process when small organic molecules are located in a condensed phase and close vicinity.[18] So it is very difficult to obtain a pretty closely packed monolayer due to the random aggregation. It is well-known that TPE and its analogues are nonplanar molecules.[18,19] When a TPE core is introduced into a molecule, it usually forms a series of propeller-like structures with a high specific surface area in the solid state. So the twisted TPE structure is expected to reduce the tendency of inactive assemblies of dyes on the semiconductor surface, extend the absorption region, and tune the HOMO and LUMO energy level. Further, the nonplanar configuration can decelerate the charge recombination in the charge-separated state and hence contribute to the improvement of the performance of DSSC.[19−21] To the best of our knowledge, there are no reports on the introduction of a twisted TPE structure into a dye molecule for DSSCs.

Among the various tactics toward the sensitizers with a high power conversion efficiency, a special interest is in the utilization of a dianchoring function group, although its initial motivation consists in enhancing the binding strength of dye molecules with TiO_2.[22] Recently, several organic sensitizers composed of two anchoring groups have been reported.[23−27] Generally speaking, the branched dianchoring approach carries a number of advantages over the unidimensional dipolar architectures: (1) larger structural variety to obtain panchro-

Received: June 5, 2015
Published: August 13, 2015

DOI: 10.1021/acs.joc.5b01140
J. Org. Chem. 2015, 80, 9034−9040

Scheme 1. Synthetic Procedures of Dyes SD and DD

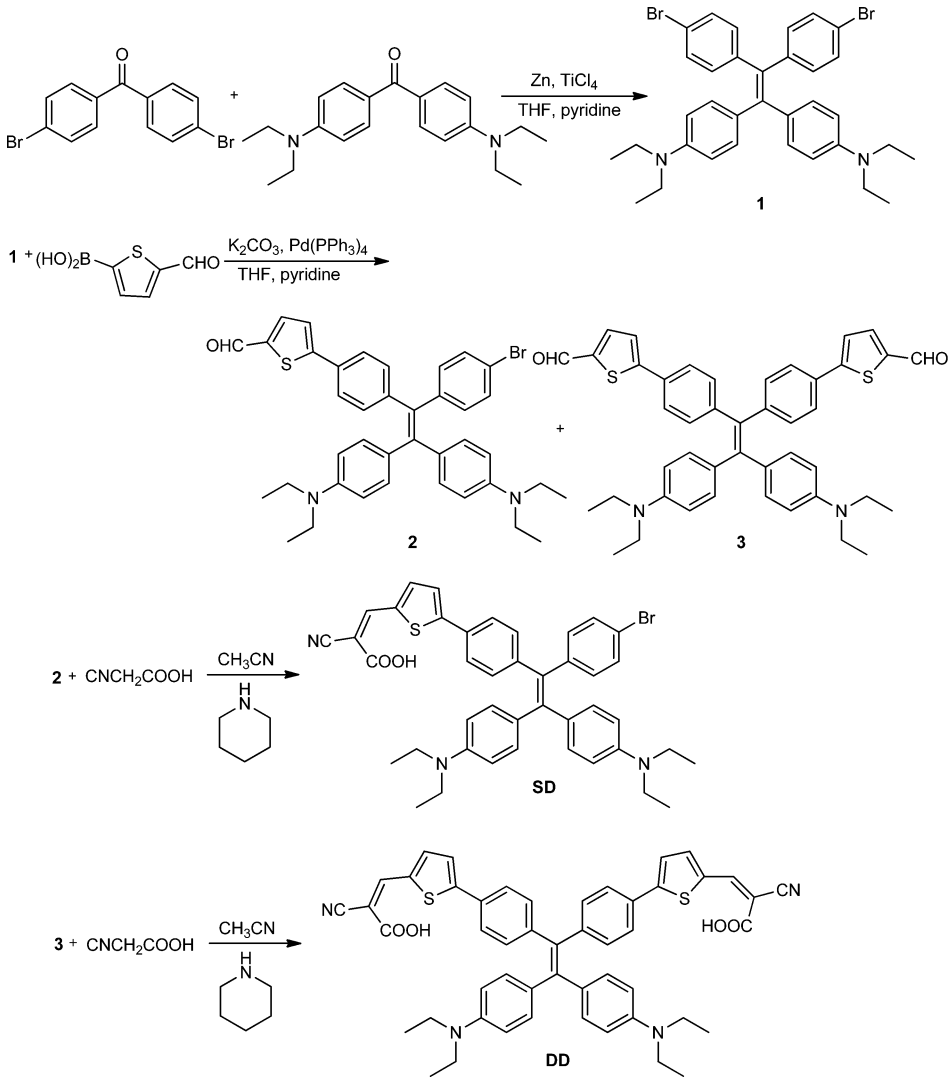

matic response; (2) enhanced optical density due to extended π-conjugated framework; and (3) multibonding to TiO_2 nanoparticles.[26−30]

In this paper, a new tailor-made dianchoring sensitizer (**DD**) featuring two DEA moieties as the donor skeleton and elaborately equipped with two cyanoacrylic acid anchoring groups at the terminal thiophene rings is synthesized for DSSC applications, which have simple structures and strong electron-donating abilities. The introduction of a twisted TPE structure into DSSC dyes is reported for the first time, which is used to induce nonplanar conformation and form a series of propeller-like structures in solid state. Further, the corresponding photosensitizer with single anchoring group (**SD**) is synthesized. The UV−vis absorption spectra, electrochemical properties, and photovoltaic parameters of DSSCs with these two dyes are extensively investigated for comparison.

RESULTS AND DISCUSSION

Synthesis. The synthetic procedures of two dyes (**SD**, **DD**) are shown in Scheme 1. The double bonds of TPE derivatives were introduced by McMurry reaction with $TiCl_4$. The aldehydes (compounds **2** and **3**) were synthesized by Suzuki coupling reaction. The dyes (**SD**, **DD**) were prepared by Knoevenagel condensation of the corresponding aldehyde with cyanoacetic acid. All the desired products were purified by column chromatography or recrystallization.

Thermal Stability. Organic sensitizers applied in DSSCs are required to possess a high thermal stability. The thermogravimetric analysis (TGA) and differential thermogravimetric (DTG) techniques were employed to investigate the thermal stability of the dyes. The decomposition temperature here is defined as the temperature at which 5% weight loss occurs during heating in nitrogen. It was found from the TGA curves (Figures S1 and S2) that the decomposition temperatures of dyes **SD** and **DD** are 274 and 313 °C, respectively. The dyes are thermally stable enough for applications in DSSCs, since the devices work usually at a temperature below 100 °C.

Photophysical Properties. The UV−vis absorption spectra of dyes **SD** and **DD** were measured in CH_2Cl_2 (Figure 1) and on TiO_2 films (Figure S3). In CH_2Cl_2, both dyes have a relatively broad and strong absorption in the ultraviolet and visible regions. The major absorption peaks for dyes **SD** and **DD** are at 270/325/388/502 nm and 371/455 nm, respectively. The absorption bands in the UV region can be assigned to a localized aromatic $\pi-\pi^*$ electron transition, while

DOI: 10.1021/acs.joc.5b01140
J. Org. Chem. 2015, 80, 9034−9040

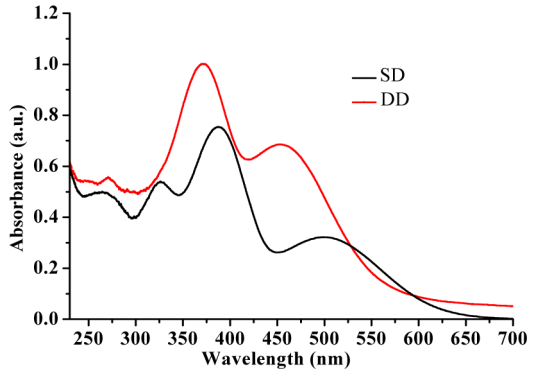

Figure 1. UV−vis spectra of dyes **SD** and **DD** in CH_2Cl_2 solution (2.0×10^{-5} mol/L).

the absorption bands in the visible region originate from an ICT transition between the DEA donor and the cyanoacrylic acid acceptor, which can produce an efficient charge-separation excited state. In comparison with dye **SD**, dye **DD** confers a broader and more intensive absorption in the ultraviolet and visible region, inducing a higher short-circuit current in DSSCs. The molar absorption coefficient (3.44×10^4 L mol^{-1} cm^{-1}) of dye **DD** is much higher than that (1.64×10^4 L mol^{-1} cm^{-1}) of dye **SD** in the range of 425−600 nm (Table 1), which is due to

Table 1. UV−vis Absorption and Electrochemical Data of the Dyes[a]

dye	$\varepsilon/10^4$ M^{-1} cm^{-1} (λ_{max}/nm)	λ_{max} on TiO_2/nm	E_{HOMO}/eV (vs. NHE)	E_{o-o}/eV	E_{LUMO}/eV[a] (vs. NHE)
SD	1.64 (502)	479	0.86	2.30	−1.44
DD	3.44 (455)	488	0.82	2.46	−1.64

[a] $E_{LUMO} = E_{HOMO} - E_{o-o}$

a higher degree of charge separation by introduction of two anchoring groups into one dye, thus, dye **DD** has a better light-harvesting ability. As shown in Figure S3, most likely due to the electronic coupling of dyes on TiO_2 surface, the UV−vis absorption spectra on TiO_2 films are broadened and red-shifts can be observed as compared with those in CH_2Cl_2.[31,32]

The fluorescence behavior of compounds **2** and **3** was studied in the diluted solutions of H_2O/THF with different H_2O fractions (Figures S4−S7). Compounds **2** and **3** have four phenyl rings with intramolecular rotations that quench their emission, however, when they turn into an aggregated form, the intramolecular coordinations occur. Accordingly, the intramolecular rotations are restricted, and the nonradiative decay channels are hindered.[18−21] As a result, these two compounds become active for emission. Plot of fluorescence emission intensity versus the different H_2O fractions in H_2O/THF mixtures shows the fluorescence behavior of compounds **2** and **3** while changing the H_2O portion of solution from 10% to 90% (Figures S5 and S7). Compounds **2** and **3** are nonemissive when dissolved in a good solvent (THF) as isolated single molecules. However, once the H_2O (a poor solvent) fraction exceeds the limit of 70%, the fluorescence intensity starts to increase drastically. So compounds **2** and **3** show the AIE property because of the TPE core.

For dyes **SD** and **DD**, a decreased intensity in the emission spectra is observed with the increase of H_2O fraction, giving an aggregation-caused emission quenching (ACEQ) effect (Figures S8−S11). The ACEQ effect of dyes **SD** and **DD** should be induced by the cyanoacrylic acid section as compounds **2** and **3** still show high AIE effect. This result could be ascribed to the solvent polarity effect and ICT state.[12,33,34] The ACEQ effect of dyes **SD** and **DD** is beneficial for the high power conversion efficiency of DSSCs because the AIE dyes can convert a portion of sunlight to the light with a longer wavelength.[12,18−20] Accordingly, the TPE structure could be introduced into organic dyes to form a propeller-like layer with a high specific surface area, but without importing the AIE property, which is helpful to improve the photovoltaic performance.

Electrochemical Data. The electrochemical properties of sensitizers are important parameters for DSSCs and can give some insight of the possibilities of electron injection from the excited dyes to the conductive band of TiO_2.[31,32] Cyclic voltammetry (CV) analyses were carried out to measure the oxidation potential (E_{ox}) (referred to as highest occupied molecular orbital (HOMO) level) of dyes. CV measurements (Figures S12−S14) indicate that the HOMO levels of dyes **SD** and **DD** are 0.86 and 0.82 eV, respectively, versus normal hydrogen electrode (NHE). Both are more positive than I^-/I_3^- redox potential value (0.3−0.4 eV vs NHE), ensuring efficient regeneration of the oxidized dye by I^- and suppressing the recapture of injected electrons by the dye cation radical. The excitation transition energy (E_{o-o}) was obtained from the intersection of the emission and absorption spectra. The LUMO levels of the two dyes (−1.44 and −1.64 eV, respectively, versus NHE, Table 1) are sufficiently more negative than the Fermi level of TiO_2 (−0.5 eV vs. NHE), suggesting a sufficient driving force is provided for the efficient electron injection into TiO_2 conduction band from the excited dyes.

Computational Modeling. To gain insight into the molecular structure and electron distribution, the geometries of dyes were optimized by density functional theory (DFT) calculations at the B3LYP/6-31G* level (Tables S1 and S2). Actually, the HOMOs of dyes **SD** and **DD** are very similar (Figure 2). They are mainly delocalized at the donor groups consisting of DEA and vinyl, with only a little extension to the phenyls. However, the LUMOs of dyes **SD** and **DD** have

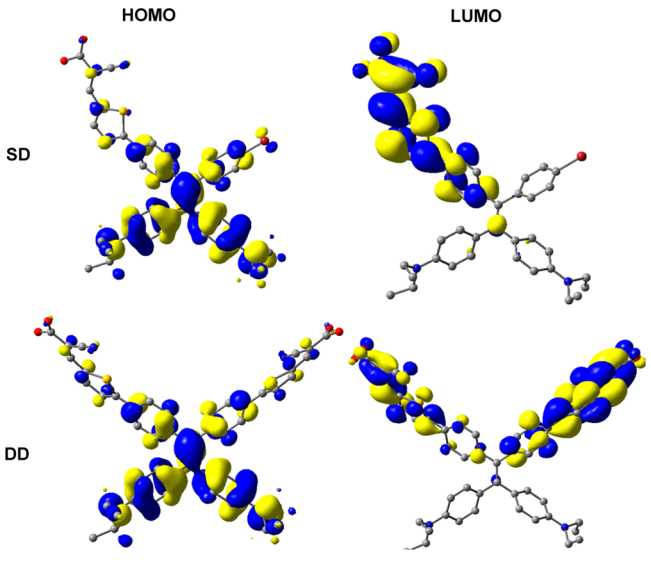

Figure 2. Frontier molecular orbitals (HOMO and LUMO) of dyes **SD** and **DD** calculated with DFT on the B3LYP/6-31G* level.

DOI: 10.1021/acs.joc.5b01140
J. Org. Chem. 2015, 80, 9034−9040

significantly different character from each other, due to the introduction of two acceptor groups, cyanoacrylic acid, into dye **DD**. The LUMO of dye **SD** delocalized only on one acceptor group, however, the LUMO of dye **DD** delocalized on two acceptor groups. As a result, the HOMO−LUMO excitation could transfer the electron distribution from the DEA donor to the cyanoacrylic acid moieties through a TPE π-conjugation bridge. However, only one acceptor group obtains the excited electron distribution in dye **SD**. As our expectation, the introduction of the second acceptor group can effectively tune the photovoltaic properties of dye **DD**. Our DFT calculation also indicated that the distance between two anchoring carboxylic acid groups of dye **DD** is 19.9 Å (Figure S31), which is close to twice the distance of two neighboring adsorption sites (10.23 Å) on the anatase TiO_2 surface.[27] So the dianchoring feature is believed to benefit the efficient surface adherence and the subsequent electron transfer. For dye **SD**, the distance between the anchoring group and Br atom is only 14.5 Å (Figure S32).

Photovoltaic Data. The photovoltaic performance characteristics of DSSCs based on dyes **DD** and **SD** under standard AM 1.5G illumination, 100 mW cm^{-2}, were summarized in Table 2. The incident monochromatic photon-to-current

Table 2. Photovoltaic Parameters of DSSCs

dye	J_{sc}/mA cm^{-2}	V_{oc}/ mv	*ff*	η(%)	τ/s	amount of dye load (mol cm^{-2})
SD	10.95	651	0.64	4.56	0.117	(4.51×10^{-7})
DD	13.20	688	0.67	6.08	0.172	(5.81×10^{-7})

conversion efficiency (IPCE) spectra of DSSCs are shown in Figure 3. Both dyes can efficiently convert visible light to

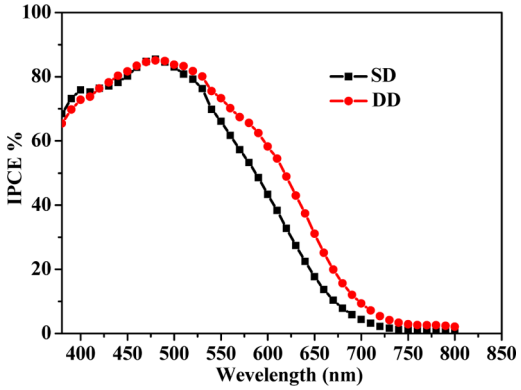

Figure 3. IPCE spectra of the DSSCs based on dyes **SD** and **DD**.

photocurrent in the region from 400 to 700 nm. The DSSCs reach an IPCE maximum of 87% around 485 nm, indicating highly efficient performance, which is due to the introduction of a TPE structure into molecules to reduce the unfavorable amorphous dye aggregation. Figure 4 shows the current density−voltage (J−V) curve of DSSCs under standard global AM 1.5 G solar irradiation. DSSCs based on dyes **SD** and **DD** give short-circuit photocurrent density (J_{sc}) of 10.95 and 13.20 mA cm^{-2}, open-circuit voltage (V_{oc}) of 651 and 688 mV, and fill factor (*ff*) of 0.64 and 0.67, corresponding to η of 4.56 and 6.08%, respectively. The better efficiency of the **DD**-sensitized DSSCs could be attributed to a higher capability of light harvesting in the visible range, evidenced by the UV−vis

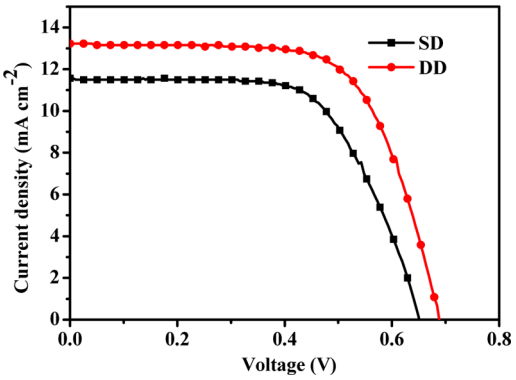

Figure 4. J−V curves of the DSSCs based on dyes **SD** and **DD**.

absorption spectra. These results indicate that the J_{sc}, V_{oc}, and *ff* can be significantly increased by the introduction of two anchoring groups into one dye molecule.

Electrochemical impedance spectroscopy (EIS) analysis was performed to elucidate the photovoltaic findings and obtain more interfacial charge transfer information (Figure 5).

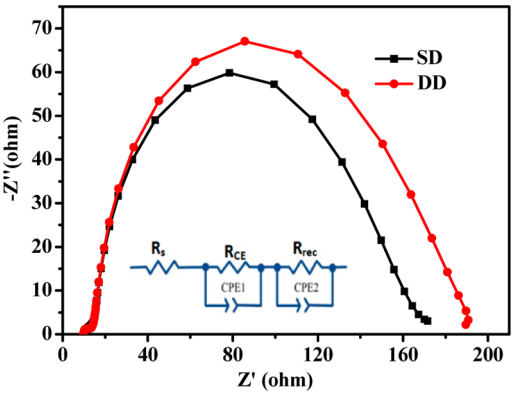

Figure 5. EIS of the DSSCs based on dyes **SD** and **DD** measured in the dark.

Impedance spectra for the cells were measured in the dark condition under a forward bias (a negative value of V_{oc} for each sample) with a frequency range of 0.1 Hz−100 kHz. Several important parameters such as the series resistance (R_S), charge-transfer resistance at the Pt/electrolyte interface (R_{CE}), and charge-transfer resistance at the TiO_2/dye/electrolyte interface (R_{rec}) were measured. The R_S values of these two cells (9.962 Ω for **SD** and 9.955 Ω for **DD**) are almost the same due to using the same electrode material and electrolyte. The small R_{CE} values (2.230 Ω for **SD** and 2.589 Ω for **DD**) mean the fast reduction of I_3^- ions at Pt counter electrode. The semicircles of Nyquist plots are assigned to R_{rec}. A lower R_{rec} value means faster electron recombination from TiO_2 to electron acceptors and thus resulting in a lower V_{oc}. Therefore, the larger semicircle radius of dye **DD** corresponds to a higher charge-transfer resistance. The electron lifetime (τ) can be calculated by fitting the equation $\tau = R_{rec} \times$ CPE (CPE, chemical capacitance), herein, τ values of 117 ms (R_{rec} = 147.3 Ω and CPE = 794.3 μF) and 172 ms (R_{rec} = 168.7 Ω and CPE = 1018.0 μF) for the DSSCs based on dyes **SD** and **DD**, respectively. The longer electron lifetime observed with the DSSCs based on dye **DD** indicates more effective suppression of the recombination of the injected electron with I^-/I_3^- in the

DOI: 10.1021/acs.joc.5b01140
J. Org. Chem. 2015, 80, 9034−9040

electrolyte, leading to an improvement in the V_{oc}. The result was also in agreement with the above observed V_{oc} value. It is well-known that the adsorption amount of dyes greatly affects the electron lifetime and V_{oc}, and therefore, the shorter lifetime of dye **SD** could be attributed to its lower dye packing density on TiO_2 (Table 2), which would result in a higher I_3^- concentration in the vicinity of TiO_2 surface and a lower charge recombination resistance. The above results indicate that the introduction of two anchoring groups into one dye can effectively improve the performance of DSSCs.

CONCLUSION

Two organic sensitizers based on a twisted TPE structure with single or double anchoring groups were synthesized. The introduction of a nonplanar TPE structure into the organic dyes for DSSCs is reported for the first time, which can form a series of propeller-like structures and reduce the tendency of dyes to randomly aggregate on TiO_2 surface. Further, the introduction of propeller-shaped TPE structure into dyes without importing the AIE property is also beneficial for the high power conversion efficiency. The dianchoring dye (**DD**) used in DSSCs led to a higher IPCE, higher J_{sc}, higher V_{oc}, longer τ and higher η as compared with the corresponding monoanchoring dye (**SD**). The results show that the performance of DSSCs could be effectively increased by introducing two anchoring groups into one molecule of dyes. This work gives some insight into how the molecular structure of organic photosensitizers affects their performances in DSSCs and sheds light on the future rational design of more powerful push−pull dyes.

EXPERIMENTAL SECTION

Materials and Measurements. All reactions were carried out under an atmosphere of argon with freshly distilled solvents, unless otherwise noted. Tetrahydrofuran (THF) and pyridine were distilled from sodium/benzophenone and CH_3CN was distilled from P_2O_5. All the other reagents were purchased from commercial sources and used without further purification unless otherwise noted. ^1H and ^{13}C NMR spectra were recorded at 25 °C on 300, 400, or 600 MHz nuclear magnetic resonance spectrometer. Chemical shifts were reported relative to Me_4Si for ^1H and ^{13}C NMR spectra. MS spectra were recorded on a matrix assisted laser desorption ionization time-of-flight mass. HRMS spectra were recorded on ESI-Q-TOF. TGA and DTG techniques were carried out from 35 to 900 °C with a heating speed of 10.0 K/min in N_2 atmosphere on a Netzsch thermogravimetric analyzer (STA449F3). CV measurements were performed on a CHI-750 electrochemical workstation (CHI Instruments, Chenhua Corporation, Shanghai, China) with a three-electrode system: a dyesensitized photoanode working electrode, a $Ag/AgNO_3$ reference electrode and a Pt plate counter electrode. All CV measurements were carried out in freshly distilled THF using tetrabutylammonium hexafluorophosphate ($TBAPF_6$, 0.1 mol/L) as the supporting electrolyte at a scan rate of 50 mVs^{-1} at room temperature, and each solution was purged with N_2 for 5 min prior to measurement. Potentials were calibrated with reference to ferrocene/ferrocenium (Fc/Fc^+, 1.0×10^{-4} mol/L) couple (0.63 eV vs NHE). The current−voltage (J−V) curves were recorded by using a Keithley 2400 source meter under simulated AM 1.5 G (100 mW/cm^2) illumination provided by a solar light simulator (Oriel, Model: 91192). A 1000 W xenon arc lamp (Oriel, Model: 6271) was used as a light source and the incident light intensity was calibrated with an NREL standard Si solar cell. The EIS measurements were performed with a Zennium electrochemical workstation (Zahner) in the dark, with an applied bias potential of a negative value of V_{oc} for each sample. A 10 mV AC sinusoidal signal was employed over the constant bias with a frequency range from 10 mHz to 1000 Hz. The impedance parameters were determined by fitting the impedance spectra with a Z-view software. The IPCE spectra were recorded on a Keithley 2000 multimeter under the illumination of a 150 W tungsten lamp with a monochromator (Spectral Product DK240). The amount of dye load was measured by desorbing the dye from the films with 0.1 M NaOH in THF/H_2O (1:1) and measuring the corresponding UV−vis spectrum.

Synthesis of Compound 1. The synthesis and spectroscopic data of compound **1** (Scheme 1) have been reported.[35] Under an Ar atmosphere, a two-necked flask equipped with a magnetic stirrer was charged with zinc dust (5 mmol, 326.95 mg, 10.0 equiv) and THF (4 mL). When the reaction mixture was cooled to −5 °C, $TiCl_4$ (2.5 mmol, 0.274 mL, 5.0 equiv) was added slowly to the reaction mixture via a syringe. The suspending mixture was warmed to room temperature and stirred for 0.5 h, then refluxed for 2.5 h. After the mixture was again cooled to −5 °C, charged with pyridine (0.3 mmol, 0.024 mL, 0.6 equiv) and stirred for 10 min. Then a THF (3 mL) solution of 4,4′-bisbromobenzophenone (0.5 mmol, 170 mg, 1.0 equiv) and 4,4′-bis(diethylamino)benzophenone (0.5 mmol, 162.23 mg, 1.0 equiv) was added slowly to the mixture. The resulting mixture was refluxed for 14.0 h. The reaction was quenched with 10% K_2CO_3 aqueous solution and extracted with dichloromethane. The extract was then dried over magnesium sulfate and filtered. After evaporation at a reduced pressure, the residue was subjected to column chromatography on silica gel (petroleum ether/ethyl acetate =30:1, v/v), affording compound **1** as solids (105 mg, 33%). ^1H NMR (400 MHz, $CDCl_3$): δ (ppm) 7.20 (d, J = 8.0 Hz, 4H), 6.88 (d, J = 8.0 Hz, 4H), 6.83 (d, J = 8.0 Hz, 4H), 6.40 (d, J = 8.0 Hz, 4H), 3.29 (q, J = 8.0 Hz, 8H), 1.12 (t, J = 8.0 Hz, 12H).

Synthesis of Compounds 2 and 3. Under an Ar atmosphere, a two-necked round flask was charged with compound **1** (0.44 mmol, 277 mg, 1.0 equiv), 5-formyl-2-thiopheneboronic (1.32 mmol, 205 mg, 3.0 equiv), K_2CO_3 (4.4 mmol, 607.2 mg, 10.0 equiv), $Pd(PPh_3)_4$ (0.044 mmol, 51 mg, 0.1 equiv), H_2O (4 mL), and THF (16 mL). After the reaction mixture was heated at 45 °C for 6.0 h, 5-formyl-2-thiopheneboronic (1.32 mmol, 205 mg, 3.0 equiv) was added to the reaction mixture again. The reaction mixture was heated at 45 °C for another 24.0 h. After reaction, H_2O (10 mL) was added to quench the reaction. The reaction mixture was extracted with dichloromethane. The extract was then dried over magnesium sulfate and filtered. After evaporation at a reduced pressure, the residue was subjected to column chromatography on silica gel (petroleum ether/dichloromethane = 1:1, v/v), affording compound **2** as red solids (125.4 mg, 43.0%) and compound **3** as red solids (156.4 mg, 51.1%), respectively. Compound **2** ^1H NMR (400 MHz, $CDCl_3$): δ (ppm) 9.85 (s, 1H), 7.69 (d, J = 4.0 Hz, 1H), 7.41 (d, J = 8.0 Hz, 2H), 7.32 (d, J = 4.0 Hz, 1H), 7.23 (d, J = 8.0 Hz, 2H), 7.07 (d, J = 8.0 Hz, 2H), 6.93 (d, J = 8.0 Hz, 2H), 6.89−6.84 (m, 4H), 6.42−6.40 (m, 4H), 3.33−3.26 (m, 8H), 1.15−1.09 (m, 12H). ^{13}C NMR (150 MHz, $CDCl_3$): δ (ppm) 182.67, 154.74, 146.95, 146.69, 146.63, 144.19, 143.58, 141.69, 137.52, 133.43, 133.31, 132.90, 132.29, 130.82, 130.35, 130.24, 129.80, 125.58, 123.48, 119.39, 110.69, 110.64, 44.15, 12.62, 12.60. MS (MALDI-TOF-TOF) m/z: $[M]^+$ Calcd for $C_{39}H_{39}BrN_2OS$ 662.196 and 664.194; Found 662.769 and 664.775. HRMS (ESI-Q-TOF) m/z: $[M + H]^+$ Calcd for $C_{39}H_{40}BrN_2OS$ 663.1994 and 665.1974; Found 663.2050 and 665.2037. Compound **3** ^1H NMR (400 MHz, $CDCl_3$): δ (ppm) 9.85 (s, 2H), 7.69 (d, J = 4.0 Hz, 2H), 7.43 (d, J = 8.0 Hz, 4H), 7.33 (d, J = 4.0 Hz, 2H), 7.11 (d, J = 8.0 Hz, 4H), 6.90 (d, J = 8.0 Hz, 4H), 6.42 (d, J = 8.0 Hz, 4H), 3.29 (q, J = 6.0 Hz, 8H), 1.11 (t, J = 6.0 Hz, 12H). ^{13}C NMR (150 MHz, $CDCl_3$): δ (ppm) 182.6, 154.7, 147.0, 146.7, 144.1, 141.7, 137.5, 133.6, 133.0, 132.3, 130.2, 129.8, 125.6, 123.5, 110.6, 44.1, 12.5. MS (MALDI-TOF-TOF) m/z: $[M]^+$ Calcd for $C_{44}H_{42}N_2O_2S_2$ 694.268; Found 694.854. HRMS (ESI-Q-TOF) m/z: $[M + H]^+$ Calcd for $C_{44}H_{43}N_2O_2S_2$ 695.2760; Found 695.2743.

Synthesis of Dye SD. Under an Ar atmosphere, a two-necked round flask was charged with compound **2** (0.2 mmol, 132.54 mg, 1.0 equiv), 2-cyanoacetic acid (0.30 mmol, 25.5 mg, 1.5 equiv), piperidine (0.30 mmol, 25.6 mg, 1.5 equiv), and CH_3CN (8 mL). The reaction mixture was heated at 100 °C for 18.0 h and cooled to room temperature. The pH value of the aqueous phase was adjusted to 2.0−3.0 with HCl (0.1 M). The reaction mixture was extracted with

DOI: 10.1021/acs.joc.5b01140
J. Org. Chem. 2015, 80, 9034−9040

dichloromethane. The extract was then dried over magnesium sulfate and filtered. After evaporation at a reduced pressure, the residue was subjected to column chromatography on silica gel (eluent: CH_2Cl_2/MeOH = 20/1, v/v), affording dye **SD** as dark red solids (116 mg, 79.3%). The product was further purified by recrystallization (petroleum ether/THF) for solar cell fabrication. ^{1}H NMR (400 MHz, $CDCl_3$): δ (ppm) 8.27 (s, 1H), 7.65 (d, J = 4.0 Hz, 1H), 7.40 (d, J = 8.0 Hz, 2H), 7.29 (d, J = 4.0 Hz, 1H), 7.23 (d, J = 8.0 Hz, 2H), 7.03−6.89 (m, 8H), 6.71 (d, J = 8.0 Hz, 2H), 6.59 (d, J = 8.0 Hz, 2H), 3.38−3.32 (m, 8H), 1.15−1.08 (m, 12H). ^{13}C NMR (100 MHz, $CDCl_3$): δ (ppm) 166.4, 152.8, 145.7, 145.0, 144.8, 143.2, 142.3, 137.7, 135.4, 135.2, 133.1, 132.9, 132.8, 132.1, 130.9, 130.4, 125.6, 123.7, 119.9, 117.5, 114.4, 112.8, 101.5, 47.0, 45.7, 12.2, 11.8. HRMS (ESI-Q-TOF) m/z: $[M + H]^+$ Calcd for $C_{42}H_{41}BrN_3O_2S$ 730.2097 and 732.2079; Found 730.2089 and 732.2066. Elemental analysis (%): calcd for $C_{42}H_{40}BrN_3O_2S$: C, 69.03; H, 5.52; N, 5.75; S, 4.39. Found: C, 69.46; H, 5.50; N, 5.82; S, 4. 46.

Synthesis of Dye DD. Under an Ar atmosphere, a two-necked round flask was charged with compound **3** (0.33 mmol, 232 mg, 1.0 equiv), piperidine (1.32 mmol, 112 mg, 4.0 equiv), cyanoacetic acid (1.32 mmol, 112 mg, 4.0 equiv), and THF (4.0 mL). The reaction mixture was heated at 85 °C for 16.0 h and cooled to room temperature. The pH value of the aqueous phase was adjusted to 2.0−3.0 with HCl (0.1 M). The reaction mixture was extracted with CH_2Cl_2. The extract was then dried over magnesium sulfate and filtered. After evaporation at a reduced pressure, the residue was washed with CH_2Cl_2 (6.0 mL) for three times. The crude product was further purified by recrystallization (petroleum ether/THF), affording compound **DD** as dark red solids (70.0 mg, 25.5%). ^{1}H NMR (300 MHz, DMSO-d_6): δ (ppm) 8.44 (s, 2H), 7.96 (d, J = 3.0 Hz, 2H), 7.67 (d, J = 3.0 Hz, 2H), 7.55 (d, J = 6.0 Hz, 4H), 7.03 (d, J = 6.0 Hz, 4H), 6.77 (d, J = 6.0 Hz, 4H), 6.41 (d, J = 6.0 Hz, 4H), 3.24 (q, J = 6.0 Hz, 8H), 1.02 (t, J = 6.0 Hz, 12H). ^{13}C NMR (100 MHz, DMSO-d_6): δ (ppm) 163.7, 152.8, 146.5, 146.4, 143.8, 141.5, 134.2, 133.5, 132.6, 132.1, 129.6, 129.5, 125.7, 124.9, 116.6, 110.5, 99.6, 98.1, 43.5, 12.5. MS (MALDI-TOF-TOF) m/z: $[M]^+$ Calcd for $C_{50}H_{44}N_4O_4S_2$ 828.280; Found 828.964. HRMS (ESI-Q-TOF) m/z: $[M + H]^+$ Calcd for $C_{50}H_{45}N_4O_4S_2$ 829.2877; Found 829.2862. Elemental analysis (%): calcd for $C_{50}H_{44}N_4O_4S_2$: C, 72.44; H, 5.35; N, 6.76; S, 7.74. Found: C, 72.46; H, 5.52; N, 6.46; S, 7.82.

Fabrication of DSSCs. DSSCs were fabricated via a reported procedure without chenodeoxycholic acid (CDCA).[36] The anatase TiO_2 nanoparticles (20 nm) were prepared through a hydrothermal method.[37] First, $Ti(OBu)_4$ (10 mL) was added to EtOH (20 mL) with stirring for 10 min. Then the mixed solvents of CH_3COOH (18 mL) and deionized H_2O (50 mL) were added to the solution with vigorous stirring for 1.0 h. The reaction mixture was heated in an autoclave at 200 °C for 12.0 h. Finally, the precipitate was washed with deionized H_2O and EtOH for five times, respectively. After being dried in air, the white TiO_2 powder (1.0 g) was ground for 40 min in a mixture of CH_3COOH (0.2 mL), EtOH (8.0 mL), ethyl cellulose (0.5 g), and terpineol (3.0 g) to form a homogeneous slurry. Finally, the slurry was sonicated for 15 min to obtain a viscous TiO_2 paste. Then the TiO_2 photoanodes (about 16 μm in thickness) were prepared via screen-printing process on the surface of fluorine-doped tin oxide (FTO) glass (7 Ω square^{-1}). The FTO glasses should be washed with detergent, H_2O, EtOH and acetone in an ultrasonic bath to remove the dirt and debris before using them. The TiO_2 films were heated through a procedure (325 °C for 5 min, 375 °C for 5 min, 450 °C for 15 min, and 500 °C for 15 min) to remove the organic substances. Then the prepared TiO_2 films were soaked in $TiCl_4$ aqueous solution (0.04 M) at 70 °C for 30 min and sintered at 520 °C for another 30 min to improve the photocurrent and photovoltaic performance. After cooling to 80 °C, the treated TiO_2 films were immersed into a CH_2Cl_2 solution of dyes (5.0×10^{-4} mol/L) for 16.0 h. Then the films were rinsed with CH_2Cl_2 to remove the physically adsorbed dye molecules. The dye-sensitized TiO_2/FTO glass films were assembled into a sandwiched type together with Pt/FTO counter electrode, which were fabricated by thermal depositing of H_2PtCl_6 solution (5 mM in isopropanol) on FTO glass at 400 °C for 15 min. The active area of the dye coated TiO_2 film was 0.16 cm^2. The electrolyte (0.6 M 1-methyl-3-propylimidazoliumiodide (PMII), 0.05 M LiI, 0.10 M guanidinium thiocyanate, 0.03 MI_2 and 0.5 M tertbutylpyridine) in an acetonitrile/valeronitrile (85:15, v/v) solution was injected into the space between the sandwiched cells from a hole on the counter electrode.

■ ASSOCIATED CONTENT

Supporting Information

The Supporting Information is available free of charge on the ACS Publications website at DOI: 10.1021/acs.joc.5b01140.

TGA and DTG curves, UV−vis spectra on TiO_2 films, fluorescence emission spectra, CV spectra, ^{1}H and ^{13}C NMR spectra, MS spectra, DFT calculation and Cartesian coordinates (PDF)

■ AUTHOR INFORMATION

Corresponding Authors

*E-mail: kuangdb@mail.sysu.edu.cn.

*E-mail: shaog@mail.sysu.edu.cn.

Notes

The authors declare no competing financial interest.

■ ACKNOWLEDGMENTS

This work was financially supported by the National Natural Science Foundation of China (21102187 and 11275090), the Natural Science Foundation of Guangdong Province (S2013010012128), and the Science and Technology Planning Project of Guangzhou City (201504291110274).

■ REFERENCES

(1) O'Regan, B.; Grätzel, M. *Nature* **1991**, *353*, 737.

(2) Hagfeldt, A.; Boschloo, G.; Sun, L. C.; Kloo, L.; Pettersson, H. *Chem. Rev.* **2010**, *110*, 6595.

(3) Hagfeldt, A.; Grätzel, M. *Acc. Chem. Res.* **2000**, *33*, 269.

(4) Mathew, S.; Yella, A.; Gao, P.; Humphry-Baker, R.; Curchod, B. F. E.; Ashari-Astani, N.; Tavernelli, I.; Rothlisberger, U.; Nazeeruddin, Md. K.; Grätzel, M. *Nat. Chem.* **2014**, *6*, 242.

(5) Numata, Y.; Singh, S. P.; Islam, A.; Iwamura, M.; Imai, A.; Nozaki, K.; Han, L. Y. *Adv. Funct. Mater.* **2013**, *23*, 1817.

(6) Hara, K.; Sato, T.; Katoh, R.; Furube, A.; Yoshihara, T.; Murai, M.; Kurashige, M.; Ito, S.; Shinpo, A.; Suga, S.; Arakawa, H. *Adv. Funct. Mater.* **2005**, *15*, 246.

(7) Kakiage, K.; Aoyama, Y.; Yano, T.; Otsuka, T.; Kyomen, T.; Unno, M.; Hanaya, M. *Chem. Commun.* **2014**, *50*, 6379.

(8) Li, J. Z.; Kong, F. T.; Wu, G. H.; Chen, W. C.; Guo, F. L.; Zhang, B.; Yao, J. X.; Yang, S. F.; Dai, S. Y.; Pan, X. *Synth. Met.* **2014**, *197*, 188.

(9) Feng, Q. Y.; Zhang, Q.; Lu, X. F.; Wang, H.; Zhou, G.; Wang, Z. S. *ACS Appl. Mater. Interfaces* **2013**, *5*, 8982.

(10) Choi, H.; Baik, C.; Kang, S. O.; Ko, J.; Kang, M. S.; Nazeeruddin, M. K.; Grätzel, M. *Angew. Chem., Int. Ed.* **2008**, *47*, 327.

(11) Mann, J. R.; Gannon, M. K.; Fitzgibbons, T. C.; Detty, M. R.; Watson, D. F. *J. Phys. Chem. C* **2008**, *112*, 13057.

(12) Chen, C. J.; Liao, J. Y.; Chi, Z. G.; Xu, B. J.; Zhang, X. Q.; Kuang, D. B.; Zhang, Y.; Liu, S. W.; Xu, J. R. *J. Mater. Chem.* **2012**, *22*, 8994.

(13) Jiao, Y.; Zhang, F.; Grätzel, M.; Meng, S. *Adv. Funct. Mater.* **2013**, *23*, 424.

(14) Cai, N.; Zhang, J.; Xu, M. F.; Zhang, M.; Wang, P. *Adv. Funct. Mater.* **2013**, *23*, 3539.

(15) Mao, J. Y.; He, N. N.; Ning, Z. J.; Zhang, Q.; Guo, F. L.; Chen, L.; Wu, W. J.; Hua, J. L.; Tian, H. *Angew. Chem., Int. Ed.* **2012**, *51*, 9873.

DOI: 10.1021/acs.joc.5b01140
J. Org. Chem. 2015, 80, 9034−9040

(16) Hagberg, D. P.; Yum, J. H.; Lee, H. J.; Angelis, F. D.; Marinado, T.; Karlsson, K. M.; Humphry-Baker, R.; Sun, L. C.; Hagfeldt, A.; Grätzel, M.; Nazeeruddin, Md. K. *J. Am. Chem. Soc.* **2008**, *130*, 6259.
(17) Zhu, W. H.; Wu, Y. Z.; Wang, S. T.; Li, W. Q.; Li, X.; Chen, J.; Wang, Z. S.; Tian, H. *Adv. Funct. Mater.* **2011**, *21*, 756.
(18) Hong, Y.; Lam, J. W. Y.; Tang, B. Z. *Chem. Soc. Rev.* **2011**, *40*, 5361.
(19) Luo, J. D.; Xie, Z. L.; Lam, J. W. Y.; Cheng, L.; Chen, H. Y.; Qiu, C. F.; Kwok, H. S.; Zhan, X. W.; Liu, Y. Q.; Zhu, D. B.; Tang, B. Z. *Chem. Commun.* **2001**, 1740.
(20) Li, Y.; Yu, H. J.; Shao, G.; Gan, F. *J. Photochem. Photobiol., A* **2015**, *301*, 14.
(21) Mei, J.; Hong, Y. N.; Lam, J. W. Y.; Qin, A. J.; Tang, Y. H.; Tang, B. Z. *Adv. Mater.* **2014**, *26*, 5429.
(22) Liu, J. Y.; Zhang, J.; Xu, M. F.; Zhou, D. F.; Jing, X. Y.; Wang, P. *Energy Environ. Sci.* **2011**, *4*, 3021.
(23) Abbotto, A.; Manfredi, N.; Marinzi, C.; Angelis, F. D.; Mosconi, E.; Yum, J. H.; Zhang, X. X.; Nazeeruddin, M. K.; Grätzel, M. *Energy Environ. Sci.* **2009**, *2*, 1094.
(24) Jiang, X.; Karlsson, K. M.; Gabrielsson, E.; Johansson, E. M. J.; Quintana, M.; Karlsson, M.; Sun, L. C.; Boschloo, G.; Hagfeldt, A. *Adv. Funct. Mater.* **2011**, *21*, 2944.
(25) Lin, L. Y.; Lu, C. W.; Huang, W. C.; Chen, Y. H.; Lin, H. W.; Wong, K. T. *Org. Lett.* **2011**, *13*, 4962.
(26) Ramkumar, S.; Manoharan, S.; Anandan, S. *Dyes Pigm.* **2012**, *94*, 503.
(27) Ting, H. C.; Tsai, C. H.; Chen, J. H.; Lin, L. Y.; Chou, S. Y.; Wong, K. T.; Huang, T. W.; Wu, C. C. *Org. Lett.* **2012**, *14*, 6338.
(28) Hong, Y. P.; Liao, J. Y.; Fu, J. L.; Kuang, D. B.; Meier, H.; Su, C. Y.; Cao, D. R. *Dyes Pigm.* **2012**, *94*, 481.
(29) Hong, Y. P.; Liao, J. Y.; Cao, D. R.; Zang, X. F.; Kuang, D. B.; Wang, L. Y.; Meier, H.; Su, C. Y. *J. Org. Chem.* **2011**, *76*, 8015.
(30) Cao, D. R.; Peng, J. A.; Hong, Y. P.; Fang, X. M.; Wang, L. Y.; Meier, H. *Org. Lett.* **2011**, *13*, 1610.
(31) Tan, L. L.; Huang, J. F.; Shen, Y.; Xiao, L. M.; Liu, J. M.; Kuang, D. B.; Su, C. Y. *J. Mater. Chem. A* **2014**, *2*, 8988.
(32) Tan, L. L.; Chen, H. Y.; Hao, L. F.; Shen, Y.; Xiao, L. M.; Liu, J. M.; Kuang, D. B.; Su, C. Y. *Phys. Chem. Chem. Phys.* **2013**, *15*, 11909.
(33) Tong, H.; Dong, Y. Q.; Häßler, M.; Hong, Y. N.; Lam, J. W. Y.; Sung, H. H. Y.; Williams, I. D.; Kwok, H. S.; Tang, B. Z. *Chem. Phys. Lett.* **2006**, *428*, 326.
(34) Hu, R. R.; Lager, E.; Aguilar-Aguilar, A.; Liu, J. Z.; Lam, J. W. Y.; Sung, H. H. Y.; Williams, I. D.; Zhong, Y. C.; Wong, K. S.; Peña-Cabrera, E.; Tang, B. Z. *J. Phys. Chem. C* **2009**, *113*, 15845.
(35) Xu, B. W.; Wu, X. F.; Li, H. B.; Tong, H.; Wang, L. X. *Macromolecules* **2011**, *44*, 5089.
(36) Zhang, H.; Fan, J.; Iqbal, Z.; Kuang, D. B.; Wang, L. Y.; Cao, D. R.; Meier, H. *Dyes Pigm.* **2013**, *99*, 74.
(37) Lei, B. X.; Fang, W. J.; Hou, Y. F.; Liao, J. Y.; Kuang, D. B.; Su, C. Y. *J. Photochem. Photobiol., A* **2010**, *216*, 8.

DOI: 10.1021/acs.joc.5b01140
J. Org. Chem. 2015, 80, 9034−9040